PAPER

Metal ion influences distortion of the ligand in the structure of [M{2-MeO(O)CC$_6$H$_4$NHC(S)NP(S)-(OiPr)$_2$}$_2$] (M = Zn^{II}, Cd^{II}) complexes: a driving force for intermolecular aggregation†‡

Damir A. Safin,*[a] Maria G. Babashkina,[a] Michael Bolte,[b] Mariusz P. Mitoraj*[c] and Axel Klein*[a]

Reaction of the *in situ* deprotonated *N*-thiophosphorylated thiourea 2-MeO(O)CC$_6$H$_4$NHC(S)NHP(S)(OiPr)$_2$ (**HL**) with MCl$_2$ (M = Zn^{II}, Cd^{II}) in aqueous ethanol leads to complexes of the formula [**ML$_2$**]. Both compounds crystallise in the triclinic space group *P*1̄ with *Z* = 2 and the metal cations are found in a tetrahedral *S$_2$S'$_2$* coordination environment formed by the C–S and P–S sulfur atoms. The crystal structures reveal intramolecular N–H···O=C hydrogen bonds formed within the 2-MeO(O)CC$_6$H$_4$NH fragments. Both structures are further stabilised by intermolecular π···π stacking interactions, which are more efficient in [**CdL$_2$**]. Here, a pronounced dimeric intermolecular aggregate is observed which goes along with a pronounced distortion of the chelate [(S)CNP(S)]$^-$ backbone of the ligand upon coordination to Cd^{II} as well as a significantly distorted coordination tetrahedron CdS$_2$S'$_2$. The aggregation is also reflected in the positive electrospray ionisation (ESI) mass spectrum of the Cd^{II} complex, which exhibits peaks for the dimeric cations [Cd$_2$L$_3$]$^+$, [Cd$_2$L$_4$ + H]$^+$ and [Cd$_2$L$_4$ + Na]$^+$, while for the Zn^{II} analogue only monomeric species were observed. Quantum chemical ETS-NOCV (ADF) calculations confirm the higher stability of dimers in [**CdL$_2$**] compared with [**ZnL$_2$**]. The π···π stacking interactions are prodominantly due to dispersion contributions, though the electrostatic and orbital interaction components are also important. QTAIM (ADF) type calculations additionally quantify the covalent and non-covalent interactions in the momomers.

Introduction

The complexation properties of imidodiphosphinate [R$_2$P(X)-NP(Y)R'$_2$]$^-$ (X, Y = O, S, Se, Te)[1] and aroylthiourea [R$_2$NC(X)-NC(Y)R']$^-$ (X, Y = O, S, Se)[2] ligands towards Zn^{II} and Cd^{II} have previously been reported. This is reflected in a total of 33 struc-

[a] Institut für Anorganische Chemie, Universität zu Köln, Greinstrasse 6, D-50939 Köln, Germany. E-mail: damir.a.safin@gmail.com, axel.klein@uni-koeln.de; Fax: +49 221 4705196; Tel: +49 221 4702913

[b] Institut für Anorganische Chemie J.-W.-Goethe-Universität, Frankfurt/Main, Germany

[c] Department of Theoretical Chemistry, Faculty of Chemistry, Jagiellonian University, R. Ingardena 3, 30-060 Cracow, Poland. E-mail: mitoraj@chemia.uj.edu.pl

tures found in the Cambridge Structural Database.[3] Recently, we have also studied the structures of Zn^{II} and Cd^{II} complexes with *N*-(thio)phosphorylated thioamidate and thioureate [RC-(S)NP(X)R'$_2$]$^-$ (X = O, S) ligands, which are asymmetric derivatives of imidodiphosphinate and aroylthiourea anions. The overwhelming majority of these structures corresponds to the phosphorylated [RC(S)NP(O)R'$_2$]$^-$ anions.[4] In contrast to this, only three structures of thiophosphorylated [RC(S)NP(S)R'$_2$]$^-$ anions are known for each Zn^{II} and Cd^{II}.[5] This is surprising since it has been postulated for a long time that complexes of the dithioderivatives are much more stable compared with those ligands containing oxygen and sulfur atoms simultaneously. Thus, every new structure of coordination compounds of [RC(S)NP(S)R'$_2$]$^-$ with Zn^{II} and Cd^{II} are of great importance and value. This becomes relevant when considering that Zn^{II} and Cd^{II} complexes with imidodiphosphinate and aroylthiourea have been extensively used as single source precursors for nanomaterials.[6] Furthermore, we have recently demonstrated that complexes of [RC(S)NP(X)R'$_2$]$^-$ with Ag^I and Ni^{II} are efficient precursors for nanoparticles and nanofilms.[7] In addition, the coordination chemistry of Zn^{II} *vs.* Cd^{II} towards

thiolate ligands receives great interest from the binding of these metals in metallothioneins.[8]

In this contribution we describe the synthesis of new Zn^{II} and Cd^{II} complexes with the N-thiophosphorylated thiourea 2-MeO(O)CC$_6$H$_4$NHC(S)NHP(S)(OiPr)$_2$ (**HL**).[9] We also describe a complete structural investigation of the obtained complexes [**ZnL$_2$**] and [**CdL$_2$**] both in solution and solid state together with their thermal properties. The experimental results were supported by detailed quantum chemical calculations.

Results and discussion

The complexes [**ZnL$_2$**] and [**CdL$_2$**] were prepared by reacting the *in situ* deprotonated ligand, using KOH, with MCl$_2$ (M = Zn^{II}, Cd^{II}) (Scheme 1). The obtained colourless solid materials are soluble in most polar solvents.

The IR spectra of complexes are very similar and contain a band at about 560 cm^{-1} representing the P–S group of the anionic form **L$^-$** with a delocalised 6 π electron S–C–N–P–S system (bond order ~1.5).[10] This band is shifted by ~90 cm^{-1} to low frequencies compared with that in the spectrum of the parent **HL**.[9] Further bands at 1530 and 1695 cm^{-1} correspond to the conjugated SCN fragment and C=O group, respectively. In addition, there is a broad intense absorption arising from the POC group at about 970–990 cm^{-1}. Also, the characteristic band for the arylNH group is found at about 3215 cm^{-1}.

The ^{31}P{^{1}H} NMR spectra of [**ZnL$_2$**] and [**CdL$_2$**] in CDCl$_3$ exhibit a unique signal at 55.7 and 55.9 ppm, respectively, which indicates the exclusive presence of 1,5-S,S'-coordinated ligands in the complexes.[9–11] The ^{1}H NMR spectra of complexes in CDCl$_3$ each contain one set of signals. The signals of the isopropyl CH$_3$ protons are observed at about 1.40 ppm, while the aryl CH$_3$ protons are at 3.90 ppm. The isopropyl CH(O) protons appear as a doublet of septets at 4.81 ppm with the characteristic coupling constants $^3J_{POCH}$ = 10.4 Hz and $^3J_{H,H}$ = 6.1 Hz. The phenylene protons are observed as four multiplet peaks at about 7.05, 7.45, 8.00 and 8.65 ppm with the typical coupling constants $^3J_{H,H}$ ranging from 7.9 to 8.3 Hz. The spectra also contain a doublet for the arylNH protons, observed at 11.25 ppm with a coupling constant $^4J_{PNCNH}$ of 7.5 Hz. The latter is exclusively observed when the structure of the H–N–C–N–P fragment meets the so-called "W-criterion" (marked by red in Scheme 1).[12] The low-field shift of the signal

for the arylNH protons is due to the formation of intra-molecular hydrogen bonds of the type arylN–H···O=C.

Crystals of the complexes were obtained by slow evaporation of the solvent from CH$_2$Cl$_2$–n-hexane solutions. Both structures represent spirocyclic chelates and were refined in the triclinic space group $P\bar{1}$, each containing one independent molecule in the unit cell. In the crystal, both Δ and Λ enantiomers of the complexes are present due to the inversion centre in the non-chiral space group $P\bar{1}$ (Fig. S1 in the ESI†). Such pairs of enantiomers can be expected for nonplanar bis-chelate complexes.[13] Both metal cations are found in a tetrahedral $S_2S'_2$ coordination environment formed by the C–S and P–S sulfur atoms (Fig. 1). The six-membered M–S–C–N–P–S metallocycles have an asymmetric boat form. The values of the endocyclic S–M–S angles are about 108.9° (Table 1) in the structure of [**ZnL$_2$**] and very close to that of the ideal tetrahedron (109.5°). The same angles in the structure of [**CdL$_2$**] deviate significantly with 101.0(1) and 104.3(1)°. The same trend is found for the exocyclic S(C)–M–S(C), S(P)–M–S(P) and S(C)–M–S(P) angles: the values fall in the range of 108.6–110.9° in the structure of
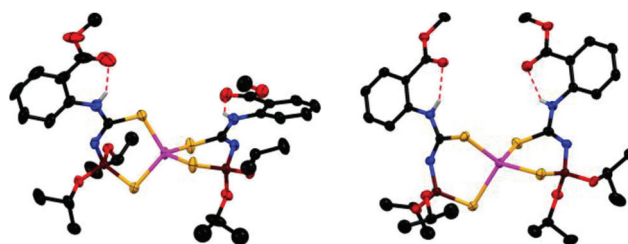

Fig. 1 Molecular structures of [**ZnL$_2$**] (left) and [**CdL$_2$**] (right). Ellipsoids are given with a 50% probability level. Hydrogen atoms not involved in H-bonding were omitted for clarity. Colour code: C = black, H = light grey, N = blue, O = red, P = brown, S = yellow, M = magenta.

Table 1 Selected bond lengths (Å), and bond angles (°) for [**ZnL$_2$**] and [**CdL$_2$**]

	[**ZnL$_2$**]	[**CdL$_2$**]
C=S	1.743(3), 1.747(2)	1.770(4), 1.778(4)
P=S	1.991(1), 1.991(1)	1.972(1), 1.992(2)
P–N	1.602(2), 1.603(2)	1.583(3), 1.604(3)
C–N(C)	1.356(3), 1.361(3)	1.342(5), 1.351(4)
C–N(P)	1.304(3), 1.305(3)	1.291(5), 1.343(5)
M–S(C)	2.3087(8), 2.3137(7)	2.433(1), 2.513(1)
M–S(P)	2.3365(7), 2.3505(7)	2.531(1), 2.621(1)
S–C–N(C)	110.5(2), 111.9(2)	111.3(3), 111.9(3)
S–C–N(P)	128.4(2), 129.2(2)	128.4(2), 128.5(3)
N–C–N	119.7(2), 120.3(2)	119.7(3), 120.2(3)
N–P–S	117.4(1), 117.5(1)	112.4(1), 119.5(1)
C–N–P	127.3(2), 128.4(2)	127.2(2), 128.5(3)
M–S–C	106.1(1), 108.9(1)	97.1(1), 101.2(1)
M–S–P	95.16(3), 97.34(3)	93.63(5), 97.71(6)
S–M–S$_{endo}$	108.89(2), 108.94(3)	101.00(5), 104.32(4)
S(C)–M–S(C)$_{exo}$	110.77(3)	116.32(4)
S(P)–M–S(P)$_{exo}$	108.71(3)	112.04(5)
S(C)–M–S(P)$_{exo}$	108.62(3), 110.85(3)	107.49(4), 115.62(4)
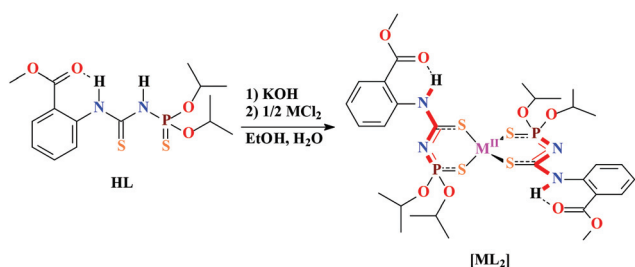
Scheme 1 Synthesis of [**ZnL$_2$**] and [**CdL$_2$**].

the Zn^{II} complex, while the corresponding values of about 116.3, 112.0, 107.5 and 115.6 were observed in the Cd^{II} analog. The two values for the N–P–S, Zn–S–C and Zn–S–P angles are very similar in [**ZnL$_2$**] representing a quite symmetric surrounding. This is not the case for [**CdL$_2$**] where the corresponding pairs show significant deviations (Table 1).

The lengthening of the C–S and P–S and shortening of the C–N(P) and P–N bonds in both complexes, compared with the values for the parent ligand **HL**,[9] are in agreement with the IR data. The relative higher symmetry of the coordination surrounding of the metal atoms in [**ZnL$_2$**] compared with [**CdL$_2$**] is also visible in the M–S(C) and M–S(P) bonds. While the each two values for the M–S(C) and M–S(P) bonds in [**ZnL$_2$**] are very similar and range from 2.31 to 2.35 Å, the two M–S(C) and M–S(P) bonds in the structure of [**CdL$_2$**] are rather dissimilar and range from 2.43 to 2.62 Å.

The arylNH protons are involved in intramolecular hydrogen bonds of the type arylN–H⋯O=C (Fig. 1 and Table 2) in line with the structure concluded from NMR (Scheme 1). A closer inspection of the crystal structures revealed further H⋯X hydrogen bonds (Table S1 in the ESI†), however, based on established criteria[14] we consider them not to be determining the crystal or molecular structures.

Both structures are further stabilised by an intermolecular π⋯π stacking interaction leading to dimers for both [**ZnL$_2$**] and [**CdL$_2$**] (Fig. 2, Table 3). The π⋯π stacking seems to be much more efficient in [**CdL$_2$**] leading to an almost coplanar arrangement (interplanar angle α = 0.03°) and a quite short interplanar distance of 3.756(3) Å with a displacement angle β of 24.12°.[15] For [**ZnL$_2$**] a second, only slightly longer, π⋯π stacking interaction (Table 3) finally leads to a 1D polymeric chain (Fig. 3), which is not observed for the Cd derivative. This marked difference seems to be caused by the pronounced distortion of the chelate [(S)CNP(S)]$^−$ fragment of the ligands upon coordination in the structure of [**CdL$_2$**] as well as the significantly distorted coordination tetrahedron CdS$_2$S$_2'$ (Fig. 4) discussed already above. Thus, the nature and especially the size of the metal cation (Zn^{II}: 74 pm *vs.* Cd^{II}: 92 pm)[16] drive the supramolecular aggregation of molecules in the structures of [**ZnL$_2$**] and [**CdL$_2$**]. A similar influence of Zn^{II} *vs.* Cd^{II} was found for the formation of supramolecular coordination complexes of the *N*-thiophosphorylated 2,5-dithiobiurea [NHC(S)-NHP(S)(OiPr)$_2$]$_2$.[5e] The dinuclear mesocate structure was formed upon reacting with Zn^{II}, while the tetranuclear nanoscaled aggregate was isolated in the reaction with Cd^{II}. Furthermore, the idea to use the different sizes of these two d^{10}
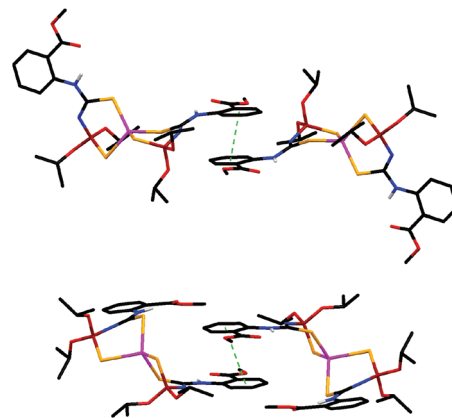

Fig. 2 Dimers formed *via* π⋯π stacking interactions in the structures of [**ZnL$_2$**] (top) and [**CdL$_2$**] (bottom). Hydrogen atoms except NH were omitted for clarity. Colour code: C = black, H = light grey, N = blue, O = red, P = brown, S = yellow, M = magenta.

Table 3 π⋯π stacking interactions for [**ZnL$_2$**] and [**CdL$_2$**]

	Cg(*I*)	Cg(*J*)	Cg–Cg (Å)	α (°)	β (°)
[**ZnL$_2$**]^a	Cg(3)	Cg(3)$^{#1}$	4.1083(15)	0.02	34.75
	Cg(4)	Cg(4)$^{#2}$	4.112(2)	0.03	32.77
[**CdL$_2$**]^b	Cg(4)	Cg(4)$^{#1}$	3.756(3)	0.03	24.12

^{a} Symmetry codes: #1 1 − x, 1 − y, 1 − z; #2 −x, −y, −z. Cg(3): C(11)–C(12)–C(13)–C(14)–C(15)–C(16), Cg(4): C(31)–C(32)–C(33)–C(34)–C(35)–C(36). ^{b} Symmetry codes: #1 1 − x, 1 − y, 1 − z. Cg(4): C(31)–C(32)–C(33)–C(34)–C(35)–C(36).
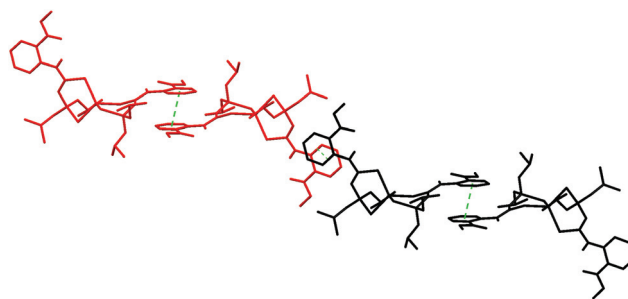

Fig. 3 1D polymeric chain formed *via* π⋯π stacking interactions of the π⋯π stacked dimers in the structure of [**ZnL$_2$**]. Hydrogen atoms except NH were omitted for clarity.

Table 2 Hydrogen bond lengths (Å) and angles (°) for [**ZnL$_2$**] and [**CdL$_2$**]

	D–H⋯A	d(D–H)	d(H⋯A)	d(D⋯A)	∠(DHA)
[**ZnL$_2$**]	N(2)–H(2)⋯O(3)	0.79(3)	2.02(3)	2.677(3)	142(3)
	N(4)–H(4)⋯O(7)	0.83(4)	1.91(4)	2.637(3)	146(3)
[**CdL$_2$**]	N(2)–H(2)⋯O(3)	0.89(4)	1.94(4)	2.680(4)	140(4)
	N(4)–H(4)⋯O(7)	0.73(4)	2.00(4)	2.620(5)	143(4)

configured so-called "spherical ions"[17] to control the supramolecular aggregation has been worked out recently.[17,18] However, in most cases the observed supramolecular aggregate is the product of several interactions and carefully ligand design is necessary.

Frequently, Cd^{II} exhibits higher coordination numbers than Zn^{II} thus changing the crystal structure.[19] It is also quite common that going from Zn^{II} to Cd^{II} leads to a higher distor-
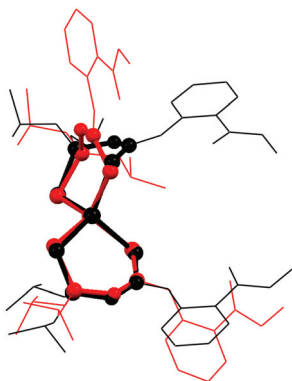
Fig. 4 Molecule overlay of **[ZnL₂]** (red) and **[CdL₂]** (black). Hydrogen atoms were omitted for clarity.

tion of the same coordination polyhedron.[5c,20] In contrast to this, the two here presented compounds represent a rare example in which the increasing size of the central metal ion well-nigh "switches on" a very strong $\pi\cdots\pi$ stacking interaction leading to a marked change in the supramolecular interactions and crystal structure; *e.g.*, the cell volume of 2006.2(2) Å³ for **[ZnL₂]** is reduced to 1949.9(7) Å³ for **[CdL₂]**.

The bulk samples of **[ZnL₂]** and **[CdL₂]** were studied by means of X-ray powder diffraction analysis (Fig. 5). The experimental X-ray powder patterns are in agreement with the calculated powder patterns obtained from a single crystal X-ray analysis, showing that the bulk materials of **[ZnL₂]** and **[CdL₂]** are free from phase impurities.

The formation of a rather stable dimeric aggregate *via* efficient intermolecular $\pi\cdots\pi$ stacking interactions is also reflected in the positive electrospray ionisation (ESI) mass spectrum of the Cd[II] complex, which exhibits intense peaks for the dimeric cations $[Cd_2L_3]^+$, $[Cd_2L_4 + H]^+$ and $[Cd_2L_4 + Na]^+$ (Fig. 6). For the Zn[II] analogue only monomeric species were found in the positive ion ESI mass spectrum.

The thermal properties of **[ZnL₂]** and **[CdL₂]** in air atmosphere were studied by means of TG analyses in order to deter-
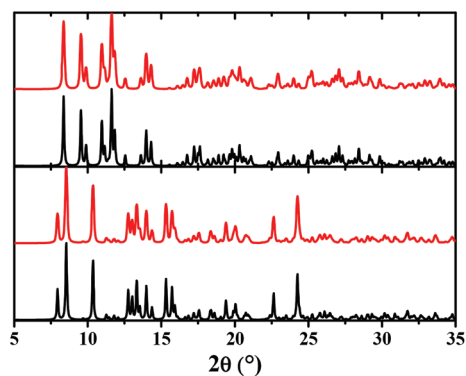

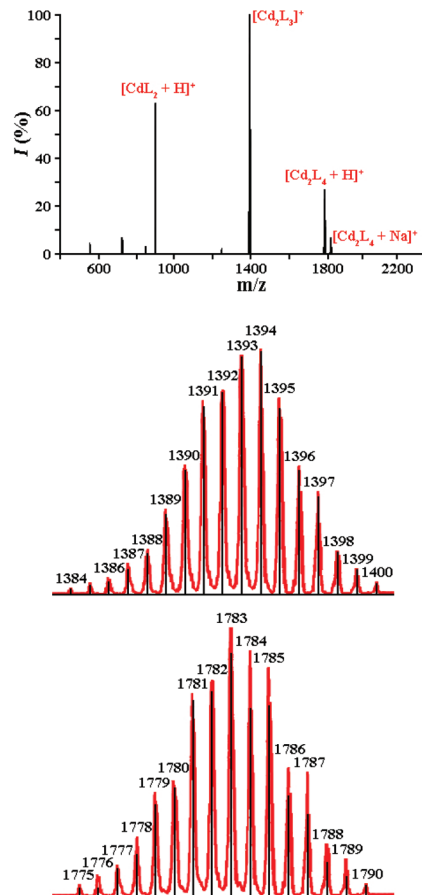**Fig. 6** The positive ion ESI-mass spectrum of **[CdL₂]** (top). Calculated (black) and experimental (red) patterns for the $[Cd_2L_3]^+$ (middle) and $[Cd_2L_4 + H]^+$ (bottom) cations.

mine their respective stabilities (Fig. 7). The compound **[ZnL₂]** is stable up to about 100 °C and decomposed in two steps. **[CdL₂]** is stable up to 140 °C and decomposed in three steps with the third step to be poorly defined. The observed final

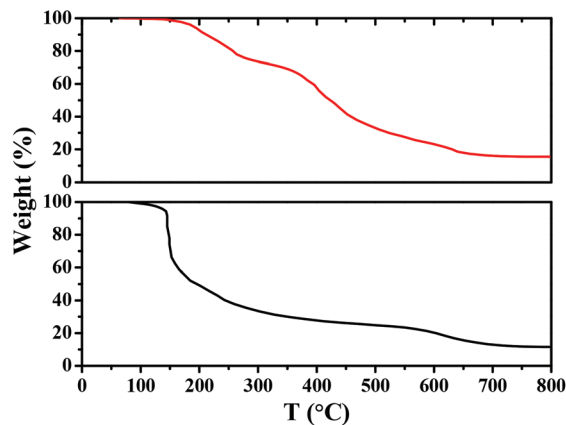**Fig. 5** Calculated (black) and experimental (red) X-ray powder diffraction patterns of **[ZnL₂]** (bottom) and **[CdL₂]** (top).

Fig. 7 TG analyses of **[ZnL₂]** (bottom) and **[CdL₂]** (top) performed in a dynamic air atmosphere.

residues of 11.6 and 16.4% are in excellent agreement with the calculated 11.54 and 16.21% for ZnS and CdS, respectively. The formation of these sulfides, each exhibiting a hexagonal form (wurtzite for ZnS and greenockite for CdS, respectively), was proved based on the powder X-ray diffraction analysis with full correspondence with data calculated from a corresponding single crystal analysis (Fig. 8).[21]

Thus, the complexes [**ZnL$_2$**] and [**CdL$_2$**], being easily obtained, and air/mosture stable might be very suitable single source precursors for the formation of ZnS and CdS, respectively.

In order to shed some light on the nature of bonding between the monomers in [**ZnL$_2$**] and [**CdL$_2$**], we have applied the charge and energy decomposition method (ETS-NOCV)[22] as implemented in the ADF2012.01 program suite.[23] We have used DFT/BLYP-D3 when performing the ETS-NOCV calculations as it was shown that such computational details provides satisfactory results for the noncovalent interactions as compared with the accurate CCSD(T) results.[24] The coordinates of the dimers were extracted from the crystal structures.

The total interaction energy (ΔE_{total}) in the dimer of [**CdL$_2$**] is significantly more pronounced compared to that of [**ZnL$_2$**] (Table 4). These results are in line with the ESI-mass spectra (Fig. 6), which also suggest a higher stability of the dimer of [**CdL$_2$**]. Decomposition of the $\pi\cdots\pi$ stacking interaction energies shows that the dispersion contribution ($\Delta E_{dispersion}$) is the

most important for the overall stabilisation and it contributes as much as −31.6 kcal mol^{-1} for [**CdL$_2$**] and −40.3 kcal mol^{-1} for [**ZnL$_2$**] (Table 4). Quantitatively less important is the electrostatic term (ΔE_{elstat}), which appeared to be quite similar for both dimers and of about −10.0 kcal mol^{-1} (Table 4). Finally, the least contribution is the orbital interaction (ΔE_{orb}), which is approximately twice more important for the cadmium-containing system. In order to shed further light on the ΔE_{orb} term we have plotted the overall deformation density ($\Delta\rho_{orb}$) upon formation of dimers (Fig. 9). The formation of both dimers leads rather to internal polarisations within the monomers, no typical charge transfer between the stacking rings is observed. It is noticeable that changes in the electron density are not only within the stacking rings but they also cover further regions including the OiPr groups as well as the sulphur atoms. The domination of the dispersion contribution in such stacking interactions is in line with the literature.[25]

We have further performed the geometry optimisation of the monomers of [**ZnL$_2$**] and [**CdL$_2$**] in the gas phase based on DFT/BLYP-D3/TZP (Fig. 10), and the calculated parameters are in qualitative agreement with the experimental values (Tables 1 and 2 and Table S2 in the ESI†).

We have finally performed a preliminary study of bonding in the monomers of [**ZnL$_2$**] and [**CdL$_2$**] based on the Quantum Theory of Atoms in Molecules (QTAIM)[26] method as implemented in the ADF program.[23] It was found that in both cases not only the strongest coordinating bonds Zn–S and Cd–S are observed, but also less important secondary intramolecular non-covalent interactions of the types O$\cdots$H–N, N$\cdots$H–C and S$\cdots$H–C. From density values at the bond critical points as well as distances one can further infer that the strength of these interactions decreases in the following order O$\cdots$H–N > N$\cdots$H–C > S$\cdots$H–C. Finally, given the fact that the
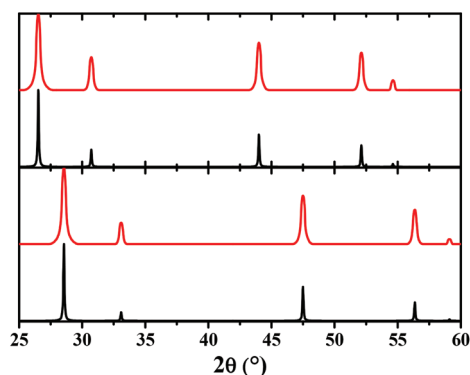

Fig. 8 Calculated (black) and experimental (red) X-ray powder diffraction patterns of ZnS (bottom) and CdS (top) obtained from annealing of [**ZnL$_2$**] and [**CdL$_2$**], respectively, at 750 °C.

Table 4 The ETS-NOCV energy decomposition results (in kcal mol^{-1}), describing $\pi\cdots\pi$ stacking interactions in dimers of [**ZnL$_2$**] and [**CdL$_2$**] based on DFT/BLYP-D3/TZP

	[**ZnL$_2$**]	[**CdL$_2$**]
ΔE_{elstat}	−9.7	−10.6
ΔE_{Pauli}	20.8	26.0
ΔE_{orb}	−4.6	−8.8
$\Delta E_{dispersion}$	−31.6	−40.3
ΔE_{total}	−25.2	−33.7

$\Delta E_{total} = \Delta E_{elstat} + \Delta E_{Pauli} + \Delta E_{orb} + \Delta E_{dispersion}$.

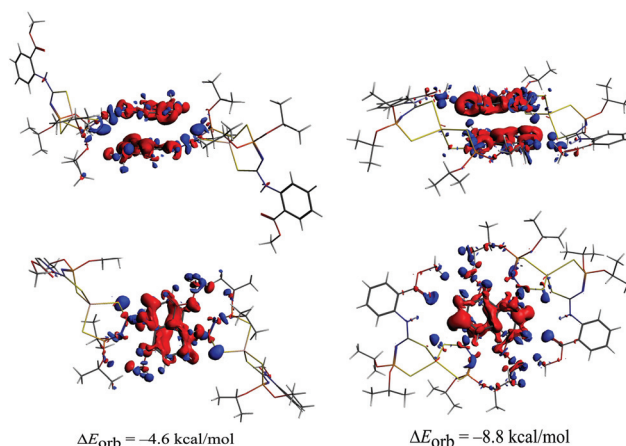$\Delta E_{orb} = -4.6$ kcal/mol $\Delta E_{orb} = -8.8$ kcal/mol

Fig. 9 Contours (0.0004 a. u.) of the overall deformation density ($\Delta\rho_{orb}$) together with the corresponding orbital interaction terms for the top (bottom) and side (top) views of dimers of [**ZnL$_2$**] (left) and [**CdL$_2$**] (right). Red colour of $\Delta\rho_{orb}$ shows the charge depletion, whereas blue colour indicates the electron density accumulation due to the formation of dimers.
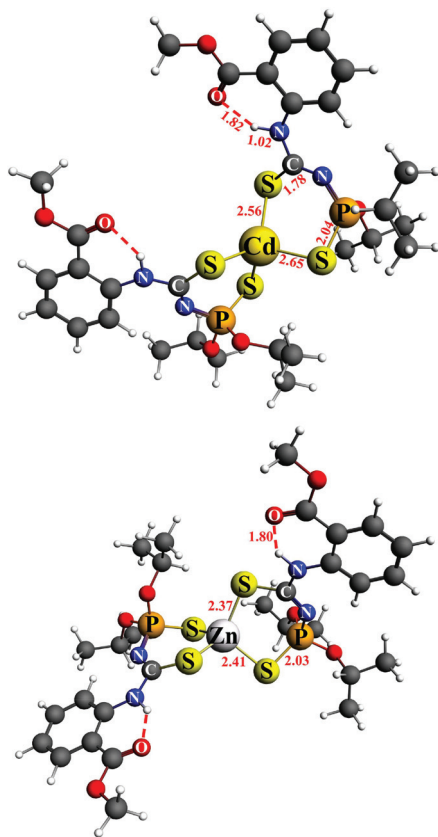
Fig. 10 The optimised structures with the selected bond lengths (Å) for monomers of [ZnL₂] (bottom) and [CdL₂] (top) based on ADF/DFT/BLYP-D3/TZP.
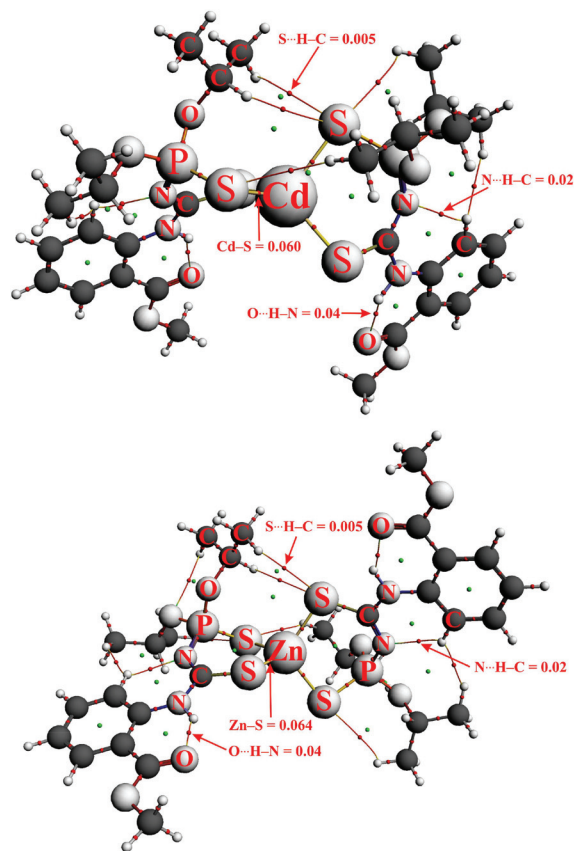

Fig. 11 The QTAIM molecular graphs together with the selected intra-molecular interactions, characterising monomers of [ZnL₂] (bottom) and [CdL₂] (top). The density values (a. u.) at the bond critical points are shown for the selected contacts.

bond critical points implies that stabilisation exists from the electronic exchange channel between atoms, further studies are required to more deeply describe each contribution of intramolecular close contacts. Nevertheless, we believe that these preliminary QTAIM based results indentify important factors that might influence the overall stability of the [ZnL₂] and [CdL₂] monomers (Fig. 11).

Conclusions

We have synthesised the Zn^{II} and Cd^{II} complexes [ZnL₂] and [CdL₂] of the deprotonated N-thiophosphorylated thiourea 2-MeO(O)CC₆H₄NHC(S)NHP(S)(OiPr)₂ (HL). The molecular structures of the complexes were studied by IR and NMR spectroscopy revealing two deprotonated ligands with a delocalised 6 π electron S–C–N–P–S system. Intramolecular N–H⋯O═C hydrogen bonds favour the all-trans arrangement of the ligands H–N–C–N–P fragment (the so-called "W-criterion"). In the solid, the structure was elucidated by single crystal X-ray diffraction analysis, revealing that both compounds crystallised isostructural in the triclinic space group P1̄, each containing one independent molecule in the unit cell. The metal cations display a tetrahedral $S_2S'_2$ coordination environment

formed by the C–S and P–S sulfur atoms and strong intra-molecular N–H⋯O═C hydrogen bonds were observed within the 2-MeO(O)CC₆H₄NH fragments. Both structures are further stabilised by intermolecular π⋯π stacking interactions, which are more efficient in [CdL₂] leading to isolated stongly connected dimers. In contrast to this, a second, weaker π⋯π stacking is observed in the Zn analogue which leads to a 1D polymeric structure in the solid. This difference between the two complexes is also reflected in the positive electrospray ionisation (ESI) mass spectrum of the Cd^{II} complex, which exhibits peaks for the dimeric cations [Cd₂L₃]⁺, [Cd₂L₄ + H]⁺ and [Cd₂L₄ + Na]⁺. Only peaks for the monomeric species were found in the ESI mass spectrum of the Zn^{II} analogue. Theoretical calculations confirm a higher stability of [CdL₂] compared with [ZnL₂]. Furthermore, the π⋯π stacking interactions are prodominantly due to dispersion contributions, though the electrostatic and orbital interaction components are also important. Thus, there is strong evidence from experiment and theory that formation of the dimeric intermolecular aggregate in the structure of [CdL₂] is driven by the pronounced distortion of the chelate [(S)CNP(S)]⁻ backbones of ligands upon coordination to Cd^{II} as well as by a significantly distorted

coordination tetrahedron CdS$_2$S'$_2$. Thus, the nature and most of all the size of the metal cation (Zn^{II} vs. Cd^{II}) drives the supramolecular aggregation of molecules in the structures of [**ZnL$_2$**] and [**CdL$_2$**].

Experimental

General procedures

Infrared spectra (Nujol) were recorded with a Thermo Nicolet 380 FT-IR spectrometer in the range 400–3600 cm^{-1}. NMR spectra in CDCl$_3$ were obtained on a Bruker Avance 300 MHz spectrometer at 25 °C. ^{1}H and ^{31}P{^{1}H} NMR spectra were recorded at 299.948, and 121.420 MHz, respectively. Chemical shifts are reported with reference to SiMe$_4$ (^{1}H) and 85% H$_3$PO$_4$ (^{31}P{^{1}H}). The electrospray ionisation (ESI) mass spectra were measured with a Finnigan-Mat TCQ 700 mass spectrometer. The speed of sample submission was 2 μL min^{-1}. The ionisation energy was 4.5 kV. The capillary temperature was 200 °C. Thermogravimetric analysis (TGA) data were recorded using a Q5000 IR TGA instrument at a heating rate of 10 °C min^{-1} between room temperature and 800 °C under a constant flow of air (100 mL min^{-1}). Elemental analyses were performed on a Thermoquest Flash EA 1112 Analyzer from CE Instruments.

DFT calculations

We have used the ADF2012.01 program[23] based on DFT/BLYP-D3/TZP. For topological description of electron density in the monomers the Quantum Theory of Atoms in Molecules (QTAIM)[26] were applied.

Synthesis of [ZnL$_2$] and [CdL$_2$]

A solution of **HL** (1 mmol, 0.390 g) in aqueous EtOH (10 mL) was mixed with KOH (1.1 mmol, 0.062 g). An aqueous (10 mL) solution of MCl$_2$ (M = Zn^{II}, Cd^{II}; 0.6 mmol, 0.082 and 0.110 g, respectively) was added dropwise under vigorous stirring to the resulting potassium salt. The mixture was stirred at room temperature for 1 h and left overnight. The resulting complex was extracted with CH$_2$Cl$_2$, washed with water and dried with anhydrous MgSO$_4$. The solvent was then removed in vacuo. Colourless crystals were isolated by recrystallisation from a 1 : 4 mixture of CH$_2$Cl$_2$ and n-hexane.

[**ZnL$_2$**]. Yield 0.388 g (92%). IR ν (cm^{-1}): 560 (P=S), 970, 987 (POC), 1531 (SCN), 1694 (C=O), 3211 (NH). ^{1}H NMR δ (ppm): 1.37 (d, $^3J_{H,H}$ = 6.2 Hz, 24H, CH$_3$, iPr), 3.92 (s, 6H, CH$_3$, Me), 4.81 (d. sept, $^3J_{POCH}$ = 10.4 Hz, $^3J_{H,H}$ = 6.1 Hz, 4H, OCH), 7.04 (d. t, $^3J_{H,H}$ = 8.2 Hz, $^4J_{H,H}$ = 1.1 Hz, 2H, p-H, C$_6$H$_4$), 7.44 (d. t, $^3J_{H,H}$ = 8.1 Hz, $^4J_{H,H}$ = 1.6 Hz, 2H, m-H, C$_6$H$_4$), 7.99 (d. d, $^3J_{H,H}$ = 8.0 Hz, $^4J_{H,H}$ = 1.5 Hz, 2H, o-H, C$_6$H$_4$), 8.65 (d, $^3J_{H,H}$ = 8.3 Hz, 2H, m-H, C$_6$H$_4$), 11.26 (d, $^4J_{PNCNH}$ = 7.4 Hz, 2H, arylNH). ^{31}P{^{1}H} NMR δ (ppm): 55.7. ES-MS positive ion, m/z (%): 454.2 (18.4) [ZnL]$^+$, 866.4 (100) [ZnL$_2$ + Na]$^+$. ES-MS negative ion, m/z (%): 389.2 (100) [L]$^-$, 1232.8 (37.2) [ZnL$_3$]$^-$. Anal. Calc. for C$_{30}$H$_{44}$N$_4$O$_8$P$_2$S$_4$Zn (844.27): C 42.68, H 5.25, N 6.64. Found: C 42.61, H 5.22, N 6.71%.

[**CdL$_2$**]. Yield 0.374 g (84%). IR ν (cm^{-1}): 558 (P=S), 970. 982 (POC), 1530 (SCN), 1695 (C=O), 3215 (NH). ^{1}H NMR δ (ppm): 1.38 (d, $^3J_{H,H}$ = 6.2 Hz, 24H, CH$_3$, iPr), 3.93 (s, 6H, CH$_3$, Me), 4.81 (d. sept, $^3J_{POCH}$ = 10.3 Hz, $^3J_{H,H}$ = 6.2 Hz, 4H, OCH), 7.04 (br. t, $^3J_{H,H}$ = 7.9 Hz, 2H, p-H, C$_6$H$_4$), 7.43 (d. t, $^3J_{H,H}$ = 8.0 Hz, $^4J_{H,H}$ = 1.4 Hz, 2H, m-H, C$_6$H$_4$), 7.98 (d. d, $^3J_{H,H}$ = 8.1 Hz, $^4J_{H,H}$ = 1.5 Hz, 2H, o-H, C$_6$H$_4$), 8.62 (d, $^3J_{H,H}$ = 8.2 Hz, 2H, m-H, C$_6$H$_4$), 11.28 (d, $^4J_{PNCNH}$ = 7.8 Hz, 2H, arylNH). ^{31}P{^{1}H} NMR δ (ppm): 55.9. ES-MS positive ion, m/z (%): 892.7 (63.4) [CdL$_2$ + H]$^+$, 1394.1 (100) [Cd$_2$L$_3$]$^+$, 1783.2 (27.1) [Cd$_2$L$_4$ + H]$^+$, 1806.7 (7.1) [Cd$_2$L$_4$ + Na]$^+$. ES-MS negative ion, m/z (%): 389.1 (100) [L]$^-$. Anal. Calc. for C$_{30}$H$_{44}$CdN$_4$O$_8$P$_2$S$_4$ (891.30): C 40.43, H 4.98, N 6.29. Found: C 40.52, H 5.06, N 6.37%.

X-Ray powder diffraction

X-Ray powder diffraction for bulk samples was carried out using a Rigaku Ultima IV X-ray powder diffractometer. The Parallel Beam mode was used to collect the data (λ = 1.541836 Å).

Single crystal X-ray diffraction

The X-ray diffraction data for the crystals of [**ZnL$_2$**] and [**CdL$_2$**] were collected at 173(2) K on a STOE IPDS-II diffractometer with graphite-monochromatised Mo-Kα radiation generated by a fine-focus X-ray tube operated at 50 kV and 40 mA. The reflections of the images were indexed, integrated and scaled using the X-Area data reduction package.[27] Data were corrected for absorption using the PLATON program.[28] The structures were solved by direct methods using the SHELXS97 program[29] and refined first isotropically and then anisotropically using SHELXL-97.[29] Hydrogen atoms were revealed from $\Delta\rho$ maps and those bonded to carbon atoms were refined using appropriate riding models. Hydrogen atoms bonded to nitrogen atoms were freely refined. All figures were generated using the program Mercury.[30]

Crystal data for [ZnL$_2$]. C$_{30}$H$_{44}$N$_4$O$_8$P$_2$S$_4$Zn, M_r = 844.24 g mol^{-1}, triclinic, space group P$\bar{1}$, a = 10.4280(5), b = 11.4053(6), c = 17.3530(9) Å, α = 78.001(4), β = 84.932(4), γ = 85.131(4)°, V = 2006.19(18) Å^3, Z = 2, ρ = 1.398 g cm^{-3}, μ(Mo-Kα) = 0.949 mm^{-1}, reflections: 32 272 collected, 7511 unique, R_{int} = 0.0510, R_1(all) = 0.0454, wR_2(all) = 0.1055.

Crystal data for [CdL$_2$]. C$_{30}$H$_{44}$CdN$_4$O$_8$P$_2$S$_4$, M_r = 891.27 g mol^{-1}, triclinic, space group P$\bar{1}$, a = 9.7368(19), b = 10.046(2), c = 21.882(4) Å, α = 97.42(3), β = 99.37(3), γ = 109.62(3)°, V = 1949.9(7) Å^3, Z = 2, ρ = 1.518 g cm^{-3}, μ(Mo-Kα) = 0.907 mm^{-1}, reflections: 18 402 collected, 7261 unique, R_{int} = 0.0853, R_1(all) = 0.0539, wR_2(all) = 0.1060.

Notes and references

1 (a) D. Cupertino, R. Keyte, A. M. Z. S. Lawin, D. J. Williams and J. D. Woollins, *Inorg. Chem.*, 1996, **35**, 2695; (b) V. Garcia-Montalvo, J. Novosad, P. Kilian, J. D. Woollins, A. M. Z. Slawin, P. Garcia y Garcia, M. Lopez-Cardoso, G. Espinosa-Perez and R. Cea-Olivares, *J. Chem. Soc., Dalton Trans.*, 1997, 1025; (c) D. C. Cupertino, R. W. Keyte,

A. M. Z. Slawin and J. D. Woollins, *Polyhedron*, 1998, **17**, 4219; (*d*) D. Cupertino, D. J. Birdsall, A. M. Z. Slawin and J. D. Woollins, *Inorg. Chim. Acta*, 1999, **290**, 1; (*e*) P. Sekar and J. A. Ibers, *Inorg. Chim. Acta*, 2001, **319**, 117; (*f*) A. Silvestru, D. Ban and J. E. Drake, *Rev. Roum. Chim.*, 2002, **47**, 1077; (*g*) M. Afzaal, D. Crouch, M. A. Malik, M. Motevalli, P. O'Brien and J.-H. Park, *J. Mater. Chem.*, 2003, **13**, 639; (*h*) M. Afzaal, D. Crouch, M. A. Malik, M. Motevalli, P. O'Brien, J.-H. Park and J. D. Woollins, *Eur. J. Inorg. Chem.*, 2004, 171; (*i*) T. Chivers, D. J. Eisler and J. S. Ritch, *Dalton Trans.*, 2005, 2675; (*j*) M. Ghesner, A. Silvestru, C. Silvestru, J. E. Drake, M. B. Hursthouse and M. E. Light, *Inorg. Chim. Acta*, 2005, **358**, 3724; (*k*) E. Ferentinos, A. B. Tsoupras, M. Roulia, S. D. Chatziefthimiou, C. A. Demopoulos and P. Kyritsis, *Inorg. Chim. Acta*, 2011, **378**, 102.

2 (*a*) W. Bensch and M. Schuster, *Z. Anorg. Allg. Chem.*, 1993, **619**, 786; (*b*) W. Bensch and M. Schuster, *Z. Anorg. Allg. Chem.*, 1993, **619**, 791; (*c*) X. Shen, X. Shi, B. Kang, Y. Liu, Y. Tong, H. Jiang and K. Chen, *Polyhedron*, 1998, **17**, 4049; (*d*) X. Shen, X. Shi, B. Kang, Y. Liu, L. Gu and X. Huang, *J. Coord. Chem.*, 1999, **47**, 1; (*e*) M. Reinel, R. Richter and R. Kirmse, *Z. Anorg. Allg. Chem.*, 2002, **628**, 41; (*f*) M. Bolte and L. Fink, Private Communication, 2003; (*g*) M. Kampf, R. Richter, L. Hennig, A. Eidner, J. Baldamus and R. Kirmse, *Z. Anorg. Allg. Chem.*, 2004, **630**, 2677; (*h*) K. E. Armstrong, J. D. Crane and M. Whittingham, *Inorg. Chem. Commun.*, 2004, **7**, 784; (*i*) H. Arslan, U. Florke, N. Kulcu and M. F. Emen, *J. Coord. Chem.*, 2006, **59**, 223; (*j*) K. Ramasamy, M. A. Malik, P. O'Brien and J. Raftery, *Dalton Trans.*, 2010, **39**, 1460; (*k*) K. Ramasamy, M. A. Malik, M. Helliwell, J. Raftery and P. O'Brien, *Chem. Mater.*, 2011, **23**, 1471.

3 *CSD version 5.35*, update February 2015th.

4 (*a*) F. D. Sokolov, D. A. Safin, N. G. Zabirov, V. V. Brusko, B. I. Khairutdinov, D. B. Krivolapov and I. A. Litvinov, *Eur. J. Inorg. Chem.*, 2006, 2027; (*b*) D. A. Safin, F. D. Sokolov, H. Nöth, M. G. Babashkina, T. R. Gimadiev, J. Galezowska and H. Kozlowski, *Polyhedron*, 2008, **27**, 2022; (*c*) D. A. Safin, M. G. Babashkina, A. Klein, M. Bolte, D. B. Krivolapov and I. A. Litvinov, *Inorg. Chem. Commun.*, 2009, **12**, 913; (*d*) D. A. Safin, A. Klein, M. G. Babashkina, H. Nöth, D. B. Krivolapov, I. A. Litvinov and H. Kozlowski, *Polyhedron*, 2009, **28**, 1504; (*e*) D. A. Safin, M. G. Babashkina, A. Klein, H. Nöth, M. Bolte and D. B. Krivolapov, *Polyhedron*, 2010, **29**, 1837; (*f*) D. A. Safin, M. G. Babashkina, M. Bolte, Ł. Szyrwiel, A. Klein and H. Kozlowski, *Phosphorus, Sulfur Silicon Relat. Elem.*, 2010, **185**, 1739; (*g*) D. A. Safin, M. G. Babashkina, M. Bolte, D. B. Krivolapov, M. L. Verizhnikov, A. R. Bashirov and A. Klein, *Inorg. Chim. Acta*, 2011, **366**, 19.

5 (*a*) D. J. Birdsall, J. Green, T. Q. Ly, J. Novosad, M. Necas, A. M. Z. Slawin, J. D. Woollins and Z. Zak, *Eur. J. Inorg. Chem.*, 1999, 1445; (*b*) N. G. Zabirov, V. V. Brusko, A. Y. Verat, D. B. Krivolapov, I. A. Litvinov and R. A. Cherkasov, *Polyhedron*, 2004, **23**, 2243; (*c*) D. A. Safin,

M. Bolte, M. G. Babashkina and H. Kozlowski, *Polyhedron*, 2010, **29**, 488; (*d*) M. G. Babashkina, D. A. Safin, M. Bolte and A. Klein, *Polyhedron*, 2010, **29**, 1515; (*e*) D. A. Safin, M. G. Babashkina, P. Kubisiak, M. P. Mitoraj, C. S. Le Duff, K. Robeyns and Y. Garcia, *Eur. J. Inorg. Chem.*, 2014, 5522.

6 For example: M. A. Malik, M. Afzaal and P. O'Brien, *Chem. Rev.*, 2010, **110**, 4417.

7 (*a*) D. A. Safin, P. S. Mdluli, N. Revaprasadu, K. Ahmad, M. Afzaal, M. Helliwell, P. O'Brien, E. R. Shakirova, M. G. Babashkina and A. Klein, *Chem. Mater.*, 2009, **21**, 4233; (*b*) M. G. Babashkina, D. A. Safin and Y. Garcia, *Dalton Trans.*, 2012, **41**, 2234; (*c*) M. G. Babashkina, D. A. Safin, K. Robeyns and Y. Garcia, *Eur. J. Inorg. Chem.*, 2015, **7**, 1160.

8 (*a*) D. E. K. Sutherland and M. J. Stillman, *Metallomics*, 2011, **3**, 444; (*b*) O. I. Leszczyszyn, H. T. Imam and C. A. Blindauer, *Metallomics*, 2013, **5**, 1146.

9 M. G. Babashkina, D. A. Safin, M. Bolte and Y. Garcia, *Dalton Trans.*, 2012, **41**, 3223.

10 (*a*) F. D. Sokolov, V. V. Brusko, N. G. Zabirov and R. A. Cherkasov, *Curr. Org. Chem.*, 2006, **10**, 27; (*b*) F. D. Sokolov, V. V. Brusko, D. A. Safin, R. A. Cherkasov and N. G. Zabirov, Coordination Diversity of N-Phosphorylated Amides and Ureas Towards VIIIB Group Cations, in *Transition Metal Chemistry: New Research*, ed. B. Varga and L. Kis, Nova Science Publishers Inc., Hauppauge NY, USA, 2008, p. 101 and references therein.

11 (*a*) M. G. Babashkina, D. A. Safin, M. Bolte and A. Klein, *Inorg. Chem. Commun.*, 2009, **12**, 678; (*b*) M. G. Babashkina, D. A. Safin, M. Bolte, M. Srebro, M. Mitoraj, A. Uthe, A. Klein and M. Köckerling, *Dalton Trans.*, 2011, **40**, 3142; (*c*) M. G. Babashkina, D. A. Safin, M. Srebro, P. Kubisiak, M. P. Mitoraj, M. Bolte and Y. Garcia, *CrystEngComm*, 2011, **13**, 5321.

12 H. Günter, *NMR Spectroscopy: An Introduction*, Wiley, Chichester, UK, 1980.

13 (*a*) A.-C. Chamayou, S. Lüdeke, V. Brecht, T. B. Freedman, L. A. Nafie and C. Janiak, *Inorg. Chem.*, 2011, **50**, 11363; (*b*) A.-C. Chamayou, G. Makhloufi, L. A. Nafie, C. Janiak and S. Lüdeke, *Inorg. Chem.*, 2015, **54**, 2193.

14 T. Steiner, *Angew. Chem., Int. Ed.*, 2002, **41**, 48.

15 C. Janiak, *J. Chem. Soc., Dalton Trans.*, 2000, 3885.

16 R. D. Shannon, *Acta Crystallogr., Sect. A: Cryst. Phys., Diffr., Theor. Gen. Cryst.*, 1976, **32**, 751.

17 (*a*) L. Bain, S. Bullock, L. Harding, T. Riis-Johannessen, G. Midgley, C. R. Rice and M. Whitehead, *Chem. Commun.*, 2010, **46**, 3496.

18 (*a*) M. Martínez-Calvo, M. J. Romero, R. Pedrido, A. M. González-Noya, G. Zaragoza and M. R. Bermejo, *Dalton Trans.*, 2012, **41**, 13395; (*b*) D. J. Cooke, J. M. Cross, R. V. Fennessy, L. P. Harding, C. R. Rice and C. Slater, *Chem. Commun.*, 2013, **49**, 7785.

19 (*a*) Q. Zhu, T. Sheng, C. Tan, S. Hu, R. Fu and X. Wu, *Inorg. Chem.*, 2011, **50**, 7618; (*b*) Y.-N. Zhang, P. Liu, Y.-Y. Wang, L.-Y. Wu, L.-Y. Pang and Q.-Z. Shi, *Cryst. Growth Des.*, 2011,

11, 1531; (*c*) M. V. Campian, I. Haiduc and E. R. T. Tiekink, *Z. Kristallogr.*, 2013, **228**, 204; (*d*) H. Zhao, D. Jia, J. Li, G. J. Moxey and C. Zhang, *Inorg. Chim. Acta*, 2015, **432**, 1; (*e*) D.-S. Liu, W.-T. Chen, Y.-P. Xu, P. Shen, S.-J. Hu and Y. Sui, *J. Solid State Chem.*, 2015, **226**, 186.

20 (*a*) A. D. Watson, C. Pulla Rao, J. R. Dorfman and R. H. Holm, *Inorg. Chem.*, 1985, **24**, 2820; (*b*) M. Saravanan, B. Arul Prakasam, K. Ramalingam, G. Bocelli and A. Cantoni, *Z. Anorg. Allg. Chem.*, 2005, **631**, 1688; (*c*) K. Baba, T. Okamura, H. Yamamoto, T. Yamamoto and N. Ueyama, *Inorg. Chem.*, 2008, **47**, 2837.

21 For example: (*a*) B. J. Skinner, *Am. Mineral.*, 1961, **46**, 1399; (*b*) C.-Y. Yeh, Z. W. Lu, S. Froyen and A. Zunger, *Phys. Rev. B: Condens. Matter*, 1992, **46**, 10086.

22 (*a*) T. Ziegler and A. Rauk, *Theor. Chim. Acta*, 1977, **46**, 1; (*b*) M. Mitoraj and A. Michalak, *J. Mol. Model*, 2007, **13**, 347; (*c*) M. P. Mitoraj, A. Michalak and T. Ziegler, *J. Chem. Theory Comput.*, 2009, **5**, 962.

23 (*a*) G. te Velde, F. M. Bickelhaupt, E. J. Baerends, C. Fonseca Guerra, S. J. A. van Gisbergen, J. G. Snijders and T. Ziegler, *J. Comput. Chem.*, 2001, **22**, 931 and references therein; (*b*) E. J. Baerends, J. Autschbach, D. Bashford, A. Bérces, F. M. Bickelhaupt, C. Bo, P. M. Boerrigter, L. Cavallo, D. P. Chong, L. Deng, R. M. Dickson, D. E. Ellis, M. van Faassen, L. Fan, T. H. Fischer, C. Fonseca Guerra, A. Ghysels, A. Giammona, S. J. A. van Gisbergen, A. W. Götz, J. A. Groeneveld, O. V. Gritsenko, M. Grüning, F. E. Harris, P. van den Hoek, C. R. Jacob, H. Jacobsen, L. Jensen, G. van Kessel, F. Kootstra, M. V. Krykunov, E. van Lenthe, D. A. McCormack, A. Michalak, M. Mitoraj, J. Neugebauer, V. P. Nicu, L. Noodleman, V. P. Osinga, S. Patchkovskii, P. H. T. Philipsen, D. Post, C. C. Pye, W. Ravenek, J. I. Rodríguez, P. Ros, P. R. T. Schipper, G. Schreckenbach, M. Seth, J. G. Snijders, M. Solà, M. Swart, D. Swerhone, G. te Velde, P. Vernooijs, L. Versluis, L. Visscher, O. Visser, F. Wang, T. A. Wesolowski, E. M. van Wezenbeek, G. Wiesenekker, S. K. Wolff, T. K. Woo, A. L. Yakovlev and T. Ziegler, *ADF2014, SCM, Theoretical Chemistry*, Vrije Universiteit, Amsterdam.

24 W. Gao, H. Feng, X. Xuan and L. Chen, *J. Mol. Model*, 2012, **18**, 4577.

25 (*a*) D. N. Sredojević, Z. D. Tomić and S. D. Zarić, *Cryst. Growth Des.*, 2010, **10**, 3901; (*b*) S. T. Mutter and J. A. Platts, *Chem. – Eur. J.*, 2010, **16**, 5391; (*c*) C. R. Martinez and B. L. Iverson, *Chem. Sci.*, 2012, **3**, 2191.

26 R. F. W. Bader, *Atoms in Molecules: A Quantum Theory*, Oxford University Press, Oxford, UK, 1990.

27 Stoe & Cie. X-AREA, *Area-Detector Control and Integration Software*, Stoe & Cie, Darmstadt, Germany, 2001.

28 A. L. Spek, *Acta Crystallogr., Sect. D: Biol. Crystallogr.*, 2009, **65**, 148.

29 G. M. Sheldrick, *Acta Crystallogr., Sect. A: Fundam. Crystallogr.*, 2008, **64**, 112.

30 I. J. Bruno, J. C. Cole, P. R. Edgington, M. Kessler, C. F. Macrae, P. McCabe, J. Pearson and R. Taylor, *Acta Crystallogr., Sect. B: Struct. Sci.*, 2002, **58**, 389.